# Generalized Multicarrier DS-CDMA Using Various Chip Waveforms

Lie-Liang Yang and Lajos Hanzo
Dept. of ECS, University of Southampton, SO17 1BJ, UK.
Tel: +44-23-8059 3125, Fax: +44-23-8059 4508
Email: lly,lh@ecs.soton.ac.uk; http://www-mobile.ecs.soton.ac.uk

***Abstract*— In this contribution the family of generalized multicarrier DS-CDMA (MC DS-CDMA) schemes [1] is investigated, when considering time-domain half-sine and raised-cosine chip waveforms, in addition to the rectangular chip waveform. Our results show that for a given subcarrier spacing the particular choice of the chip waveform has a substantial influence on the system's performance. However, in the context of MC DS-CDMA using the optimum subcarrier spacing, all chip waveforms may provide a similar bit error rate (BER) performance.**

## I. Introduction

In reference [1], [2] a generalized MC DS-CDMA scheme using rectangular chip waveforms has been investigated, when communicating over frequency-selective Nakagami-$m$ fading channels [3]. As argued in [1], [2], in generalized MC DS-CDMA the spacing between two adjacent subcarriers is a variable, allowing us to gain insight into the effects of the subcarrier spacing on the BER performance. This generalized MC DS-CDMA scheme includes the subclasses of multitone DS-CDMA [4] and orthogonal MC DS-CDMA [5] as special cases.

In this contribution we extend our investigations presented in [1] by considering two additional chip waveforms, namely the time-domain half-sine as well as the raised-cosine chip waveforms, in addition to the rectangular chip waveform. We derive the second-order statistics for the multipath interference (MPI) or multiuser interference (MUI), when the subcarrier signals are partially overlapped. A range of closed-form equations are obtained in the context of various chip waveforms. These closed-form equations allow us to evaluate the BER performance of CDMA systems using overlapping subbands [1],[4]-[7] with the aid of the standard Gaussian approximation.

## II. Received Signals and Decision Variables

In [1] we considered an asynchronous generalized MC DS-CDMA scheme, which supports $K$ users transmitting over dispersive frequency-selective Nakagami-$m$ fading channels. The received signal is expressed as [1]

$$r(t)=\sum_{k=1}^{K}\sum_{u=1}^{U}\sum_{l_p=0}^{L_p-1}\sqrt{2P}\alpha_{ul_p}^{(k)}b_{ku}(t-\tau_{kl_p})c_k(t-\tau_{kl_p})\times\cos\left(2\pi f_u t+\theta_{ul_p}^{(k)}\right)+n(t), \quad (1)$$

where the following notations are used:

- $K$: the number of users
- $U$: the number of subcarriers
- $f_u$: the $u$th subcarrier frequency
- $T_s$: symbol duration of the MC DS-CDMA signal
- $T_c$: chip duration of the DS spreading sequences associated with each subcarrier
- $N_e=T_s/T_c$: spreading gain of each subcarrier signal
- $n(t)$: Additive White Gaussian Noise (AWGN) having double-sided power spectral density of $N_0/2$
- $P$: average received power of each subcarrier signal
- $L_p$: the number of resolvable paths of each subcarrier conveying a DS-CDMA signal
- $\alpha_{ul_p}^{(k)}$: Nakagami-$m$ distributed channel fading amplitude [[1], (9)]
- $\tau_{kl_p}$: multipath signal delay associated with asynchronous transmission and propagation, which is an independently and identically distributed (i.i.d) uniform variable in $[0,T_s]$
- $\theta_{ul_p}^{(k)}$: phase angle introduced in the carrier modulation and propagation processes, which is an i.i.d uniform variable in $[0,2\pi]$
- $b_{ku}(t)$: binary data stream's waveform
- $c_k(t)=\sum_{j=-\infty}^{\infty}c_{kj}\psi(t-jT_c)$: binary spreading sequence's waveform, where $\psi(t)$ is the chip waveform.

Let the first user associated with $k=1$ be the user-of-interest and consider the correlator-based RAKE receiver in conjunction with maximum ratio combining (MRC) [1]. We assume that the first $L$, $1\le L\le L_p$ number of resolvable paths are combined by the receiver. Consequently, as shown in [1], the decision variable $Z_v$ of the 0th data bit corresponding to the $v$th subcarrier of the reference user can be expressed as

$$Z_v = \sum_{l=0}^{L-1} Z_{vl},\ v=1,2,\ldots,U, \quad (2)$$

$$Z_{vl} = \int_{\tau_l}^{T_s+\tau_l} r(t)\cdot\alpha_{vl}c(t-\tau_l)\cos\left(2\pi f_v t+\theta_{vl}\right)dt, \quad l=0,1,\ldots,L-1, \quad (3)$$

where $Z_{vl}$ is the correlator's output corresponding to the $l$th resolvable path of the $v$th subcarrier. Upon substituting (1) into (3), it can be shown that $Z_{vl}$ can be written as

$$Z_{vl}=\sqrt{\frac{P}{2}}T_s\left\{D_{vl}+N_{vl}+\sum_{\substack{l_p=0\\ l_p\neq l}}^{L_p-1}I_1^{(s)}+\sum_{\substack{u=1\\ u\neq v}}^{U}\sum_{\substack{l_p=0\\ l_p\neq l}}^{L_p-1}I_2^{(s)}+\sum_{k=2}^{K}\sum_{l_p=0}^{L_p-1}I_1^{(k)}+\sum_{k=2}^{K}\sum_{\substack{u=1\\ u\neq v}}^{U}\sum_{l_p=0}^{L_p-1}I_2^{(k)}\right\}, \quad (4)$$

where $N_{vl}$ is a Gaussian random variable having zero mean and a variance of $\alpha_{vl}^2N_0/2E_b$, with $E_b=PT_s$ denoting the energy per bit, while $D_{vl}=b_v[0]\alpha_{vl}^2$ is the desired output. Furthermore, in (4) $Z_{vl}$ contains four types of interference:

This work has been funded in the framework of the IST project IST-2001-34091 SCOUT, which is partly funded by the European Union. The authors would like to acknowledge the contributions of their colleagues.

- $I_1^{(s)}$ is the MPI contributed by the path $l_p,\ l_p = 0, 1, \ldots, L_p - 1$ and $l_p \neq l$ of the reference user associated with $k = 1$, and with the same subcarrier of index $u = v$ as the reference user.
- $I_2^{(s)}$ is the MPI contributed by the path $l_p,\ l_p = 0, \ldots, L_p - 1,\ l_p \neq l$, associated with the subcarriers $u,\ u = 1, 2, \ldots, U,\ u \neq v$ of the reference user.
- $I_1^{(k)}$ is the MUI due to the path $l_p,\ l_p = 0, 1, \ldots, L_p - 1$ associated with the subcarrier $u = v$ engendered by the interfering users, $k = 2, 3, \ldots, K$.
- $I_2^{(k)}$ is the MUI due to the path $l_p,\ l_p = 0, \ldots, L_p - 1$ induced by the subcarrier $u,\ u = 1, \ldots, U$ and $u \neq v$ of the interfering user $k,\ k = 2, 3, \ldots, K$.

Since random spreading sequences and encountering an arbitrary spacing of $\Delta = \lambda/T_s$ between two adjacent subcarriers were assumed, it can be demonstrated that $I_1^{(s)}$, $I_2^{(s)}$ and $I_1^{(k)}$ constitute special cases of $I_2^{(k)}$, where $I_2^{(k)}$ can be expressed as [1]

$$I_2^{(k)} = \frac{\alpha_{ul_p}^{(k)} \alpha_{vl}}{T_s} \Big[ b_{ku}[-1] R_k(\tau_{kl_p}, \varphi_{ul_p}^{(k)}, u, v) + b_{ku}[0] \hat{R}_k(\tau_{kl_p}, \varphi_{ul_p}^{(k)}, u, v) \Big], \quad (5)$$

where $\varphi_{ul_p}^{(k)} = \theta_{ul_p}^{(k)} - \theta_{vl}$ is a random variable uniformly distributed in $[0, 2\pi]$. The associated partial cross-correlation functions in (5) are defined as [1]

$$R_k(\tau_{kl_p}, \theta_{ul_p}^{(k)}, u, v) = \int_0^{\tau_{kl_p}} c_k(t - \tau_{kl_p}) c(t) \times \cos\left( \frac{2\pi\lambda(u-v)t}{T_s} + \varphi_{ul_p}^{(k)} \right) dt, \quad (6)$$

$$\hat{R}_k(\tau_{kl_p}, \theta_{ul_p}^{(k)}, u, v) = \int_{\tau_{kl_p}}^{T_s} c_k(t - \tau_{kl_p}) c(t) \times \cos\left( \frac{2\pi\lambda(u-v)t}{T_s} + \varphi_{ul_p}^{(k)} \right) dt. \quad (7)$$

## III. Interference Analysis

In this section we investigate the statistical properties of $I_2^{(k)}$ using the Gaussian approximation [8]. Where possible without any danger of ambiguity, we ignore the superscript and subscript associated with the delay $\tau_{kl_p}$ and the phase angle $\varphi_{kl_p}^{(k)}$ for the sake of simplicity. Based on the standard Gaussian approximation [8], [7], it was shown that for a given $\alpha_{vl}$ value, the MUI term $I_2^{(k)}$ of (5) can be approximated as a Gaussian random variable having zero mean and a variance given by

$$\text{Var}\left[ I_2^{(k)} \right] = \Omega_{ul_p}^{(k)} \alpha_{vl}^2 \mathcal{I}_2^{(k)}, \quad (8)$$

where $\Omega_{ul_p}^{(k)} = E\left[ \left( \alpha_{ul_p}^{(k)} \right)^2 \right]$, and

$$\mathcal{I}_2^{(k)} = \frac{1}{T_s^2} \left\{ E_{\tau,\varphi}\left[ R_k^2(\tau, \varphi, u, v) \right] + E_{\tau,\varphi}\left[ \hat{R}_k^2(\tau, \varphi, u, v) \right] \right\}, \quad (9)$$

where $E_{\tau,\varphi}\left[ R_k^2(\tau, \varphi, u, v) \right]$ and $E_{\tau,\varphi}\left[ \hat{R}_k^2(\tau, \varphi, u, v) \right]$ constitute the second central-moments of $R_k(\tau, \varphi, u, v)$ and $\hat{R}_k(\tau, \varphi, u, v)$ with respect to $\tau$ and $\varphi$. Furthermore, it can be readily demonstrated that we have $E_{\tau,\varphi}\left[ R_k^2(\tau, \varphi, u, v) \right] = E_{\tau,\varphi}\left[ \hat{R}_k^2(\tau, \varphi, u, v) \right]$, when random spreading sequences are considered. It can be shown that $E_{\tau,\varphi}\left[ R_k^2(\tau, \varphi, u, v) \right]$ can be expressed as

$$E_{\tau,\varphi}\left[ R_k^2(\tau, \varphi, u, v) \right] = \frac{(N_e + 1)}{2} E_{\tau_c,\varphi}\left[ R_\psi^2(\tau_c, \varphi, u, v) \right] + \frac{(N_e - 1)}{2} E_{\tau_c,\varphi}\left[ \hat{R}_\psi^2(\tau_c, \varphi, u, v) \right], \quad (10)$$

where $E_{\tau_c,\varphi}\left[ R_\psi^2(\tau_c, \varphi, u, v) \right]$ and $E_{\tau_c,\varphi}\left[ \hat{R}_\psi^2(\tau_c, \varphi, u, v) \right]$ represent the second central moments of the *extended* partial autocorrelation functions $R_\psi(\tau_c, \varphi, u, v)$ and $\hat{R}_\psi(\tau_c, \varphi, u, v)$ of the spreading codes, with respect to $\tau_c$ and $\varphi$, respectively. The extended partial autocorrelation functions are defined as

$$R_\psi(\tau_c, \varphi, u, v) = \int_0^{\tau_c} \psi(t)\psi(t + T_c - \tau_c) \times \cos\left( \frac{2\pi\lambda(u-v)t}{T_s} + \varphi \right), \quad (11)$$

$$\hat{R}_\psi(\tau_c, \varphi, u, v) = \int_{\tau_c}^{T_c} \psi(t)\psi(t - \tau_c) \times \cos\left( \frac{2\pi\lambda(u-v)t}{T_s} + \varphi \right). \quad (12)$$

Below the expectation values of $E_{\tau_c,\varphi}\left[ R_\psi^2(\tau_c, \varphi, u, v) \right]$ and $E_{\tau_c,\varphi}\left[ \hat{R}_\psi^2(\tau_c, \varphi, u, v) \right]$ corresponding to three different classes of chip waveforms, namely rectangular, half-sine and raised-cosine chip waveforms are derived.

Since both $\tau_c$ and $\varphi$ are uniform random variables distributed in the range of $[0, T_c]$ and $[0, 2\pi]$, respectively, the expectation value of $E_{\tau_c,\varphi}\left[ R_\psi^2(\tau_c, \varphi, u, v) \right]$ can be expressed as

$$E_{\tau_c,\varphi}\left[ R_\psi^2(\tau_c, \varphi, u, v) \right] = \frac{1}{2\pi T_c} \int_0^{T_c} \int_0^{2\pi} R_\psi^2(\tau_c, \varphi, u, v) d\varphi d\tau_c, \quad (13)$$

$$E_{\tau_c,\varphi}\left[ \hat{R}_\psi^2(\tau_c, \varphi, u, v) \right] = \frac{1}{2\pi T_c} \int_0^{T_c} \int_0^{2\pi} \hat{R}_\psi^2(\tau_c, \varphi, u, v) d\varphi d\tau_c. \quad (14)$$

Upon substituting Equations (11) and (12) defined in the context of the rectangular, half-sine and raised-cosine chip waveforms into equations (13) as well as (14) and following a number of laborious but straightforward manipulations, we obtain the following results.

(I). **Rectangular Chip Waveform**

If $\lambda(u - v) \neq 0$, then we have

$$E_{\tau_c,\varphi}\left[ R_\psi^2(\tau_c, \varphi, u, v) \right] = E_{\tau_c,\varphi}\left[ \hat{R}_\psi^2(\tau_c, \varphi, u, v) \right] = \frac{T_s^2}{4\pi^2\lambda^2(u-v)^2} \left[ 1 - \text{sinc}\left( \frac{2\pi\lambda(u-v)}{N_e} \right) \right]. \quad (15)$$

By contrast, if we have $\lambda(u - v) = 0$, then we arrive at

$$E_{\tau_c,\varphi}\left[ R_\psi^2(\tau_c, \varphi) \right] = E_{\tau_c,\varphi}\left[ \hat{R}_\psi^2(\tau_c, \varphi) \right] = \frac{T_c^2}{6}. \quad (16)$$

(II). **Half-Sine Chip Waveform**

If $|\lambda(u-v)| \neq 0, N_e$, then we get

$$
\begin{aligned}
&E_{\tau_c,\varphi}\left[R_\psi^2(\tau_c,\varphi,u,v)\right] = E_{\tau_c,\varphi}\left[\hat{R}_\psi^2(\tau_c,\varphi,u,v)\right] \\
&= \frac{T_s^2}{8\pi^2} \\
&\times \Bigg[\frac{1}{\lambda^2(u-v)^2} + \frac{1}{2[N_e+\lambda(u-v)]^2} + \frac{1}{2[N_e-\lambda(u-v)]^2} \\
&\quad - \frac{1}{\lambda(u-v)[N_e+\lambda(u-v)]} + \frac{1}{\lambda(u-v)[N_e-\lambda(u-v)]} \\
&\quad - \Bigg(\frac{1}{\lambda^2(u-v)^2} - \frac{1}{\lambda(u-v)\,[N_e+\lambda(u-v)]} \\
&\qquad + \frac{1}{\lambda(u-v)\,[N_e-\lambda(u-v)]} \\
&\qquad - \frac{1}{N_e^2-\lambda^2(u-v)^2}\Bigg)\,\mathrm{sinc}\left(\frac{2\pi\lambda(u-v)}{N_e}\right) \\
&\quad - \Bigg(\frac{1}{2\lambda^2(u-v)^2} + \frac{1}{2[N_e+\lambda(u-v)]^2} \\
&\quad - \frac{1}{\lambda(u-v)[N_e+\lambda(u-v)]}\Bigg)\,\mathrm{sinc}\left(\frac{2\pi[N_e+\lambda(u-v)]}{N_e}\right) \\
&\quad - \Bigg(\frac{1}{2\lambda^2(u-v)^2} + \frac{1}{2[N_e-\lambda(u-v)]^2} \\
&\quad + \frac{1}{\lambda(u-v)[N_e-\lambda(u-v)]}\Bigg)\,\mathrm{sinc}\left(\frac{2\pi[N_e-\lambda(u-v)]}{N_e}\right)\Bigg]. \quad (17)
\end{aligned}
$$

If however $\lambda(u-v)=0$, then we have

$$
E_{\tau_c,\varphi}\left[R_\psi^2(\tau_c,\varphi)\right] = E_{\tau_c,\varphi}\left[\hat{R}_\psi^2(\tau_c,\varphi)\right] = T_c^2\left(\frac{1}{12}+\frac{5}{8\pi^2}\right). \quad (18)
$$

Finally, if $|\lambda(u-v)| = N_e$, then we arrive at

$$
\begin{aligned}
E_{\tau_c,\varphi}\left[R_\psi^2(\tau_c,\varphi)\right] &= E_{\tau_c,\varphi}\left[\hat{R}_\psi^2(\tau_c,\varphi)\right] \\
&= T_c^2\left(\frac{1}{24}+\frac{5}{64\pi^2}\right). \quad (19)
\end{aligned}
$$

(III). **Raised-cosine Chip Waveform**

If $|\lambda(u-v)| \neq 0, N_e, 2N_e$, then we have

$$
\begin{aligned}
&E_{\tau_c,\varphi}\left[R_\psi^2(\tau_c,\varphi,u,v)\right] = E_{\tau_c,\varphi}\left[\hat{R}_\psi^2(\tau_c,\varphi,u,v)\right] \\
&= \frac{T_s^2}{72\pi^2} \\
&\quad \times \Bigg[\Bigg(\frac{9}{\lambda^2(u-v)^2} + \frac{4}{[N_e+\lambda(u-v)]^2} + \frac{4}{[N_e-\lambda(u-v)]^2} \\
&\qquad + \frac{1}{2[2N_e+\lambda(u-v)]^2} + \frac{1}{2[2N_e-\lambda(u-v)]^2} \\
&\qquad - \frac{10}{\lambda(u-v)[N_e+\lambda(u-v)]} \\
&\qquad + \frac{10}{\lambda(u-v)[N_e-\lambda(u-v)]} + \frac{1}{\lambda(u-v)[2N_e+\lambda(u-v)]} \\
&\qquad - \frac{1}{\lambda(u-v)[2N_e-\lambda(u-v)]} - \frac{4}{N_e^2-\lambda^2(u-v)^2} \\
&\qquad - \frac{2}{[N_e+\lambda(u-v)][2N_e+\lambda(u-v)]} \\
&\qquad - \frac{2}{[N_e-\lambda(u-v)][2N_e-\lambda(u-v)]}\Bigg) \\
&\qquad - \Bigg(\frac{9}{\lambda^2(u-v)^2} + \frac{2}{[N_e+\lambda(u-v)]^2} + \frac{2}{[N_e-\lambda(u-v)]^2} \\
&\qquad - \frac{10}{\lambda(u-v)[N_e+\lambda(u-v)]} + \frac{10}{\lambda(u-v)[N_e-\lambda(u-v)]} \\
&\qquad + \frac{1}{\lambda(u-v)[2N_e+\lambda(u-v)]} - \frac{1}{\lambda(u-v)[2N_e-\lambda(u-v)]} \\
&\qquad - \frac{8}{N_e^2-\lambda^2(u-v)^2} + \frac{2}{[N_e+\lambda(u-v)][2N_e-\lambda(u-v)]} \\
&\qquad + \frac{2}{[N_e-\lambda(u-v)][2N_e+\lambda(u-v)]} \\
&\qquad - \frac{1}{[4N_e^2-\lambda^2(u-v)^2]}\Bigg)\,\mathrm{sinc}\left(\frac{2\pi\lambda(u-v)}{N_e}\right) \\
&\qquad - \Bigg(\frac{4}{\lambda^2(u-v)^2} + \frac{4}{[N_e+\lambda(u-v)]^2} - \frac{10}{\lambda(u-v)[N_e+\lambda(u-v)]} \\
&\qquad + \frac{2}{\lambda(u-v)[N_e-\lambda(u-v)]} + \frac{4}{\lambda(u-v)[2N_e+\lambda(u-v)]} \\
&\qquad - \frac{4}{[N_e^2-\lambda^2(u-v)^2]} - \frac{2}{[N_e+\lambda(u-v)][2N_e+\lambda(u-v)]} \\
&\qquad + \frac{2}{[N_e-\lambda(u-v)][2N_e+\lambda(u-v)]}\Bigg)\,\mathrm{sinc}\left(\frac{2\pi[N_e+\lambda(u-v)]}{N_e}\right) \\
&\qquad - \Bigg(\frac{4}{\lambda^2(u-v)^2} + \frac{4}{[N_e-\lambda(u-v)]^2} + \frac{10}{\lambda(u-v)[N_e-\lambda(u-v)]} \\
&\qquad - \frac{2}{\lambda(u-v)[N_e+\lambda(u-v)]} - \frac{4}{\lambda(u-v)[2N_e-\lambda(u-v)]} \\
&\qquad - \frac{4}{[N_e^2-\lambda^2(u-v)^2]} + \frac{2}{[N_e+\lambda(u-v)][2N_e-\lambda(u-v)]} \\
&\qquad - \frac{2}{[N_e-\lambda(u-v)][2N_e-\lambda(u-v)]}\Bigg)\,\mathrm{sinc}\left(\frac{2\pi[N_e-\lambda(u-v)]}{N_e}\right) \\
&\qquad - \Bigg(\frac{1}{2\lambda^2(u-v)^2} + \frac{2}{[N_e+\lambda(u-v)]^2} + \frac{1}{2[2N_e+\lambda(u-v)]^2} \\
&\qquad - \frac{2}{\lambda(u-v)[N_e+\lambda(u-v)]} + \frac{1}{\lambda(u-v)[2N_e+\lambda(u-v)]} \\
&\qquad - \frac{2}{[N_e+\lambda(u-v)][2N_e+\lambda(u-v)]}\Bigg)\,\mathrm{sinc}\left(\frac{2\pi[2N_e+\lambda(u-v)]}{N_e}\right) \\
&\qquad - \Bigg(\frac{1}{2\lambda^2(u-v)^2} + \frac{2}{[N_e-\lambda(u-v)]^2} + \frac{1}{2[2N_e-\lambda(u-v)]^2} \\
&\qquad + \frac{2}{\lambda(u-v)[N_e-\lambda(u-v)]} - \frac{1}{\lambda(u-v)[2N_e-\lambda(u-v)]} \\
&\qquad - \frac{2}{[N_e-\lambda(u-v)][2N_e-\lambda(u-v)]}\Bigg) \\
&\qquad \times \mathrm{sinc}\left(\frac{2\pi[2N_e-\lambda(u-v)]}{N_e}\right)\Bigg]. \quad (20)
\end{aligned}
$$

By contrast, if $\lambda(u-v)=0$, then we have

$$
\begin{aligned}
E_{\tau_c,\varphi}\left[R_\psi^2(\tau_c,\varphi)\right] &= E_{\tau_c,\varphi}\left[\hat{R}_\psi^2(\tau_c,\varphi)\right] \\
&= T_c^2\left(\frac{1}{12}+\frac{315}{864\pi^2}\right). \quad (21)
\end{aligned}
$$

Furthermore, if $|\lambda(u-v)| = N_e$, then we get

$$
E_{\tau_c,\varphi}\left[R_\psi^2(\tau_c,\varphi)\right] = E_{\tau_c,\varphi}\left[\hat{R}_\psi^2(\tau_c,\varphi)\right]
$$

$$= \quad T_c^2 \left( \frac{1}{27} + \frac{35}{162\pi^2} \right). \qquad (22)$$

Finally, if $|\lambda(u-v)| = 2N_e$, then we arrive at

$$\begin{aligned} E_{\tau_c,\varphi}\left[R_\psi^2(\tau_c,\varphi)\right] &= E_{\tau_c,\varphi}\left[\hat{R}_\psi^2(\tau_c,\varphi)\right] \\ &= T_c^2\left(\frac{1}{216} + \frac{245}{20736\pi^2}\right). \end{aligned} \qquad (23)$$

Finally, based on the above second central-moment values of the partial autocorrelation functions with respect to the rectangular, half-sine and raised-cosine chip waveforms, the corresponding expectation values in $E_{\tau,\varphi}\left[R_k^2(\tau,\varphi,u,v)\right]$ of (10) as well as $E_{\tau,\varphi}\left[\hat{R}_k^2(\tau,\varphi,u,v)\right] = E_{\tau,\varphi}\left[R_k^2(\tau,\varphi,u,v)\right]$ can be obtained. Upon substituting these expectation values into (8) and (9), the variance of $\mathcal{I}_2^{(k)}$ and $I_2^{(k)}$ corresponding to the rectangular, half-sine or raised-cosine chip waveforms can be evaluated. Specifically, for the case of $\lambda(u-v) = 0$, we have

$$\begin{aligned} \mathcal{I}_2^{(k)} &= \mathcal{I}_1^{(k)} = \mathcal{I}_1^{(s)} \\ &= \mathcal{I}_0 = \begin{cases} \frac{1}{3N_e}, & \text{Rectangular} \\ \frac{1}{6N_e} + \frac{5}{4N_e\pi^2}, & \text{Half-sine} \\ \frac{1}{6N_e} + \frac{315}{432N_e\pi^2}, & \text{Raised-cosine} \end{cases} \end{aligned} \qquad (24)$$

which are some of the typical MUI variance values valid in the context of single-carrier DS-CDMA schemes.

## IV. Bit Error Rate

Having obtained the statistics of both the MPI as well as the MAI, and furthermore, following the approach of [1], the average BER of the generalized MC DS-CDMA system communicating over multipath Nakagami-$m$ fading channels can be expressed as

$$P_b = \frac{1}{\pi}\int_0^{\pi/2} \prod_{l=0}^{L-1} \left( \frac{m\sin^2\theta}{\overline{\gamma}_l + m\sin^2\theta} \right)^m d\theta, \qquad (25)$$

where $m$ represents the fading parameter [3], $\overline{\gamma}_l = \gamma_c e^{-\eta l}$ for $l = 0, 1, \ldots, L-1$, $\eta$ is the Multipath Intensity Profile's (MIP) negative exponential decay factor and $\gamma_c$ is expressed as

$$\gamma_c = \left[ \left( \frac{\Omega_0 E_b}{N_0} \right)^{-1} + \frac{2(KL_p - 1)q(L_p,\eta)}{L_p} \left( \mathcal{I}_0 + (U-1)\overline{\mathcal{I}}_M \right) \right]^{-1}, \qquad (26)$$

where $\mathcal{I}_0$ is given by (24), while $\overline{\mathcal{I}}_M$ represent the average of $\mathcal{I}_2^{(k)}$ with respect to $v$ and $u$, which can be expressed as

$$\overline{\mathcal{I}}_M = \frac{1}{U(U-1)} \sum_{v=1}^{U} \sum_{\substack{u=1 \\ u\neq v}}^{U} \mathcal{I}_2^{(k)}. \qquad (27)$$

## V. Numerical Results

In this section we characterize the effects of the spacing between two subcarriers on the interference power and evaluate the performance of generalized MC DS-CDMA by highlighting the effect of the normalized subcarrier spacing, $\lambda$, on the system's performance.

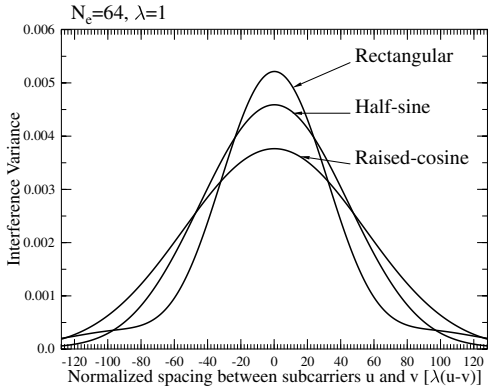


Fig. 1. Interference power $\mathcal{I}_2^{(k)}$ of (9) versus the normalized spacing, $\lambda(u-v)$ between two subcarrier frequencies $f_u$ and $f_v$ with respect to the rectangular, half-sine as well as raised-cosine chip waveforms.

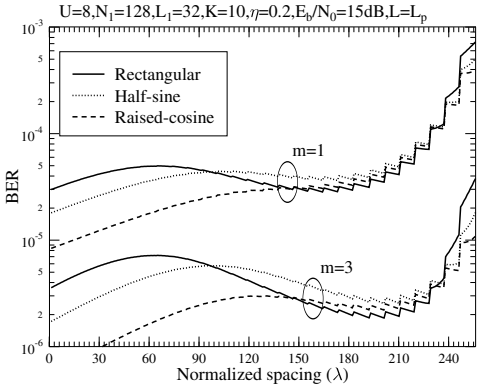


Fig. 2. BER versus the normalized subcarrier spacing, $\lambda$ for the generalized MC DS-CDMA system communicating over the multipath Nakagami-$m$ fading channel using the fading parameters of $m = 1$ and $m = 3$. The results were computed from (25) by assuming that $L = L_p$, i.e. that the receiver was capable of combining all the resolvable paths, regardless of the associated receiver complexity.

Fig.1 gives us an insight into the interference behaviour for different chip waveforms associated with different subcarrier spacings. Let us assume that $f_v$ is one of the subcarrier frequencies of the reference signal, while $f_u$ is one of the subcarrier frequencies used by the interfering signals. According to the results of Fig.1, we observe that for all the chip waveforms considered, the interference power decreases, when increasing the absolute subcarrier spacing value of $|\lambda(u-v)|$. If we have $\lambda(u-v) = 0$, which implies that $f_u = f_v$, the spreading sequences using a rectangular chip waveform impose the highest interference power, while using a raised-cosine chip waveform results in the lowest interference power. When increasing the subcarrier spacing $|\lambda(u-v)|$, we can observe that there exists a spacing range, where the rectangular chip waveform outperforms both the half-sine and the raised-cosine chip waveforms. The results of Fig.1 demonstrate that

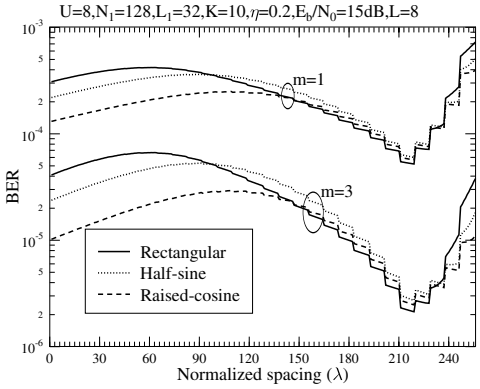


Fig. 3. BER versus the normalized subcarrier spacing, $\lambda$ for the generalized MC DS-CDMA system communicating over the multipath Nakagami-$m$ fading channel using the fading parameters of $m = 1$ and $m = 3$. The results were computed from (25) by assuming that the maximum multipath combining capability was $L = 8$, i.e. that the receiver was capable of combining at most eight resolvable paths due to implementation complexity limitations.

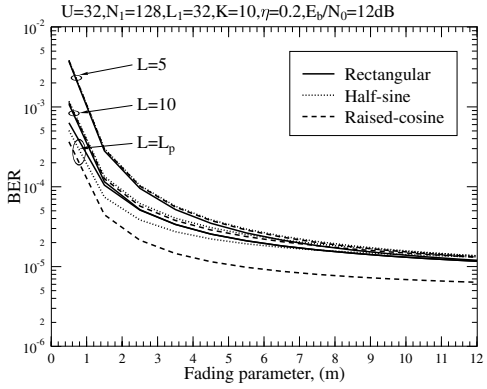


Fig. 4. BER versus the fading parameter, $m$, for MC DS-CDMA having the optimum normalized subcarrier spacing and using rectangular, half-sine as well as raised-cosine chip waveforms, when communicating over multipath Nakagami-$m$ fading channels. The results were computed from (25) by assuming that the maximum multipath combining capability was $L = 5, 10$ or $L = L_p$.

the interference power at the point of $\lambda(u - v) = 0$ is more than twenty times higher, than that at the point of $\lambda(u - v) = 2N_e = 128$. Therefore, we can infer that in a MC DS-CDMA system, the MPI and the MUI are mainly contributed by the specific subcarrier signals having overlapping main lobes.

The influence of the normalized subcarrier spacing, $\lambda$, on the average BER of the generalized MC DS-CDMA system is shown in Fig.2 and Fig.3, where we assumed Nakagami fading parameters of $m = 1$ and 3. In the context of Fig.2 we assumed that the receiver was capable of combining all the resolvable paths, i.e. we had $L = L_p$, regardless of the implementing complexity. By contrast, we assumed that the receiver was capable of combining at most $L = 8$ resolvable paths in Fig.3, owing to implementing receiver complexity limit. At the top of Figs.2 and 3 $N_1$ and $L_1$ represent the spreading gain and the number of resolvable paths of a corresponding conventional single-carrier DS-CDMA scheme using the same total bandwidth, as the proposed MC DS-CDMA arrangement.

From the results of Fig.2 we infer that the multicarrier system using both the half-sine and the raised-cosine chip waveforms achieved their lowest BER at low normalized subcarrier spacing values of $\lambda$, while single-carrier DS-CDMA associated with $\lambda = 0$ achieved the best BER performance. However, the multicarrier system using the rectangular chip waveform might not achieve its lowest BER, when the normalized spacing value is low, especially for channels having relatively high Nakagami fading parameters, since the associated BER curve has its minimum value in the range of $\lambda \approx 180 - 210$. According to the results of Fig.3, we observe that for each of the chip waveforms considered, there exists an optimum value of $\lambda$, which will result in the minimum average BER. The optimum value of $\lambda$ was similar for all three types of chip waveforms, which was around $\lambda = 215$. Furthermore, from the results of both Figs.2 and 3 we observe that when the normalized spacing of $\lambda$ assumes a sufficiently high value, the MC DS-CDMA systems using any of the three chip waveforms studied achieved a similar BER performance.

In Fig.4 the BER performance versus the fading parameter, $m$ recorded for the MC DS-CDMA system having the optimum subcarrier spacing was evaluated, when employing rectangular, half-sine and raised-cosine chip waveforms, respectively. From the results of Fig.4 we observe that for the diversity combining capability of $L = 5$ and 10, the MC DS-CDMA systems using the rectangular, half-sine or raised-cosine chip waveform achieved a similar BER performance, when communicating over channels having arbitrary Nakagami fading parameters. However, if the receiver was capable of combining an arbitrary number of resolvable paths, i.e. when we had $L = L_p$, we observe that the system using the raised-cosine chip waveform outperforms both that using the rectangular and the half-sine chip waveforms. We can also see in Fig.4 that the scheme employing the half-sine chip waveform outperforms that using the rectangular chip waveform, when the Nakagami fading factor is in the range of $m \leq 7$. By contrast, both of them achieve a similar BER performance, when we have $m > 7$.

## REFERENCES


[1] L.-L. Yang and L. Hanzo, "Performance of generalized multicarrier DS-CDMA over Nakagami-$m$ fading channels," *IEEE Trans. on Commun.*, vol. 50, pp. 956 – 966, June 2002.

[2] L.-L. Yang and L. Hanzo, "A unified approach to the analysis of multicarrier DS-CDMA over Nakagami-$m$ fading channels," in *Proc. of IEEE GLOBECOM*, (San Antonio, Texas, USA), Nov. 25-29, 2001.

[3] M.-S. A. Marvin K. Simon, *Digital Communication over Fading Channels: A Unified Approach to Performance Analysis*. New York: John Wiley & Sons, 2000.

[4] L. Vandendorpe, "Multitone spread spectrum multiple access communications system in a multipath Rician fading channel," *IEEE Trans. on Veh. Tech.*, vol. 44, no. 2, pp. 327–337, 1995.

[5] E. A. Sourour and M. Nakagawa, "Performance of orthogonal multicarrier CDMA in a multipath fading channel," *IEEE Trans. on Commun.*, vol. 44, pp. 356–367, March 1996.

[6] M. A. Laxpati and J. W. Gluck, "Optimization of hybrid SFH/DS MFSK link in the presence of worst case multitone jamming," *IEEE Trans. on Commun.*, vol. 43, pp. 2118–2156, June 1995.

[7] L.-L. Yang and L. Hanzo, "Overlapping $M$-ary frequency shift keying SSMA systems using random signature sequences," *IEEE Trans. on Veh. Tech.*, vol. 48, pp. 1984–1995, November 1999.

[8] M. B. Pursley, "Performance evaluation for phase-coded spread-spectrum multiple-access communication-Part I: System analysis," *IEEE Trans. on Commun.*, vol. COM-25, pp. 795–799, Aug. 1977.